

Effect of Fuselage Geometry on Delta-Wing Vortex Breakdown

Lars E. Ericsson*
Mountain View, California 94040

A fuselage is usually associated with the use of a delta wing on an actual aircraft. It is also in many cases necessary to use a centerbody of some shape in tunnel tests of pure delta wings. The present paper describes the flow physics causing the experimentally observed large effect of a fuselage on delta-wing vortex breakdown.

Nomenclature

B	= deflection angle of apex flap, Fig. 6
b	= wingspan
c	= wing root chord
l	= rolling moment, coefficient $C_l = l/(\rho_\infty U_\infty^2/2)Sb$
p	= static pressure, coefficient $C_p = (p - p_\infty)/(\rho_\infty U_\infty^2/2)$
Re	= Reynolds number based on c and freestream conditions
S	= reference area, projected wing area
U	= horizontal velocity
W_{LE}	= body-induced upwash effect at the leading edge
x	= chordwise coordinate, distance from apex
α	= angle of attack
Δ	= increment
$\Delta\alpha_{LE}$	= angular delay of leading-edge flow separation, Eq. (1)
δ_{LE}	= angle of leeside leading-edge bevel
Λ	= leading-edge sweep
ξ	= dimensionless x coordinate, x/c
ρ	= air density
σ	= inclination of the roll axis
ϕ	= roll angle

Subscripts

B	= vortex breakdown
eff	= effective
LE	= leading edge
∞	= freestream conditions

Introduction

THE purpose of the original test¹ of the configuration shown in Fig. 1 was to demonstrate that the high-alpha aerodynamics of delta wings are so nonlinear that locally linearized analysis cannot be applied, creating the need for new methods to describe and use experimental results.² With this fact established, numerous experimental and theoretical investigations followed, in which the effect of the presence of the centerbody (Fig. 1) never was seriously considered. It is the purpose of the present paper to demonstrate that this effect is large and cannot be neglected in any realistic analysis.

Analysis

In tests of the 65-deg delta-wing-body configuration^{1,3} (Fig. 1), the vortex breakdown location varied with alpha as shown

in Fig. 2, occurring significantly aft of the location measured by others⁴ for a pure 65-deg delta wing. The angle of attack for the results in Fig. 2a need to be corrected for the effect of the leeside bevel angle δ_{LE} at the leading edge.⁵ The effective angle of attack is

$$\alpha_{\text{eff}} = \alpha - \Delta\alpha_{LE}, \quad \Delta\alpha_{LE} = \tan^{-1}(\tan \delta_{LE} \cos \Lambda) \quad (1)$$

When the test results in Fig. 2a are plotted against the effective angle of attack α_{eff} , corrected for the effect of δ_{LE} , 7.5 deg for W & K and 10 deg for H & H, it becomes evident that the fuselage had a large effect on vortex breakdown in the H & H test (Fig. 2b).³ The L & B data have not been corrected. Together with the large bevel angle $\delta_{LE} = 16$ deg, one also has to consider that the wing was seven times thicker than the others. As pointed out in Ref. 4, the all-important apex flow conditions are very sensitive to wing thickness. There are presently no simple means available for considering the combined effect of leading-edge bevel and wing thickness. At $\alpha = 30$ deg, the breakdown on the delta-wing-body configuration³ (Fig. 1) occurs more than 30% chord aft of the breakdown locations on the pure delta wings.⁴

Body-Induced Camber Effect

The presence of a centerbody has been shown to have a large effect on vortex breakdown on a 69.33-deg delta wing⁶ (Fig. 3). However, in this case, the effect was to promote vortex breakdown to occur much earlier than for a pure delta wing, not much later (Fig. 2), as the case was for the fuselage geometry shown in Fig. 1. Following a suggestion by Tobak,[†] that the fuselage effect could be defined more clearly than in Ref. 7 by considering "The analogy ... between forms of pressure distribution induced on the one hand by streamwise camber and on the other hand by wing-body interference" and "the introduction of a deformable planar wing surface to make the logic clear," the fuselage effect in Fig. 3 is now derived as follows. Figure 4a illustrates how the body-induced upwash along the leading edge would vary without the delta wing in place, and Fig. 4b shows how the same flow conditions along the leading edge could be generated by the planar delta wing alone if it were given the appropriate negative streamwise camber. As demonstrated by the experimental results by Lambourne and Bryer⁹ (Fig. 5b), the negative camber will promote vortex breakdown, in agreement with the experimental results⁶ in Fig. 3. If instead of being a circular cylinder the centerbody had an ogival shape, the fuselage-induced upwash along the leading edge without the wing in place would vary as illustrated in Fig. 6a. For each cylindrical segment in the approximation of the ogival body shape, the upwash distribution

Received Jan. 15, 1997; revision received March 5, 1998; accepted for publication Aug. 10, 1998. Copyright © 1998 by Lars E. Ericsson. Published by the American Institute of Aeronautics and Astronautics, Inc., with permission.

*Engineering Consultant. Fellow AIAA.

†Tobak, M., private communication, Mountain View, CA, Feb. 1998.

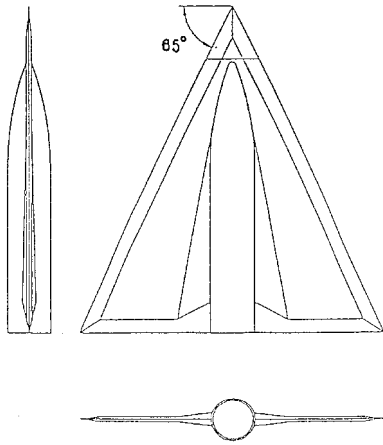
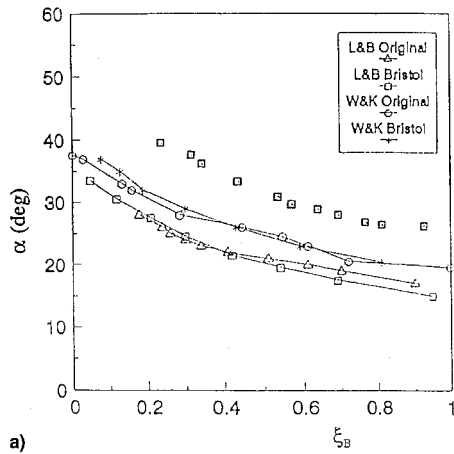
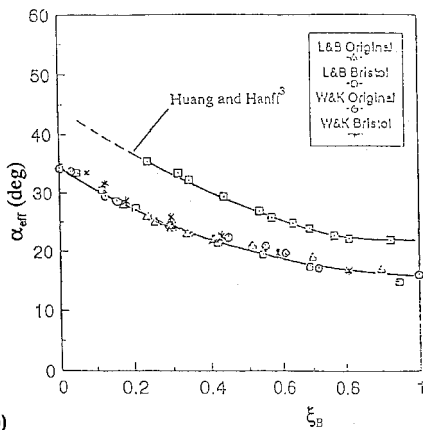


Fig. 1 Tested 65-deg delta-wing-body geometry.¹



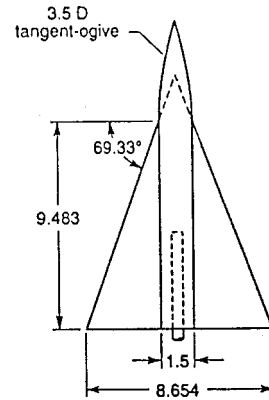
a)



b)

Fig. 2 Measured breakdown location on a 65-deg delta-wing-body configuration³ compared with that on pure 65-deg delta wings⁴: a) original results, $\xi_B = f(\alpha)$ and b) results corrected for the effect of leading-edge level, $\xi_B = f(\alpha_{eff})$.

would be that shown in Fig. 4a. In the limit of an infinite number of cylindrical segments, the continuous upwash distribution indicated by the dashed line would result. Figure 6b shows the cambered, planar delta wing that will generate the same flow conditions at the leading edge as those generated by the centerbody in Fig. 6a. Thus, the tested wing-body configuration (Figs. 1 and 7a) can be represented by the cambered pure delta-wing geometry sketched in Fig. 7b. According to the experimental results⁸ in Fig. 5, the positive camber on the forward part of the wing would delay vortex breakdown (Fig. 5a), and the negative camber on the aft part would promote breakdown (Fig. 5b). Apparently, according to the experi-



	Re	Λ_w	Wing	Reference
●	1.8×10^4	69.3°	Wing-body	Present work
■	2.2×10^4	69.3°	Wing-alone	Present work
○	3.0×10^4	70.0°		Erickson
□	4.0×10^5	70.0°		Roos & Kegelman
◇	4.3×10^5	70.0°		Payne
△	1.0×10^6	70.0°		Wentz & Kohlman
▽	1.3×10^6	69.3°		Brennenstuhl & Hummel

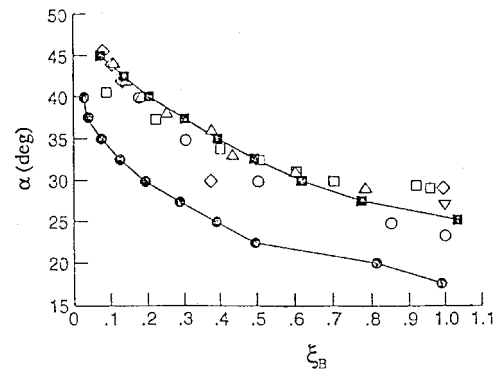


Fig. 3 Effect of cylindrical centerbody on $\xi_B = f(\alpha)$ on a 69.33-deg delta wing.⁶

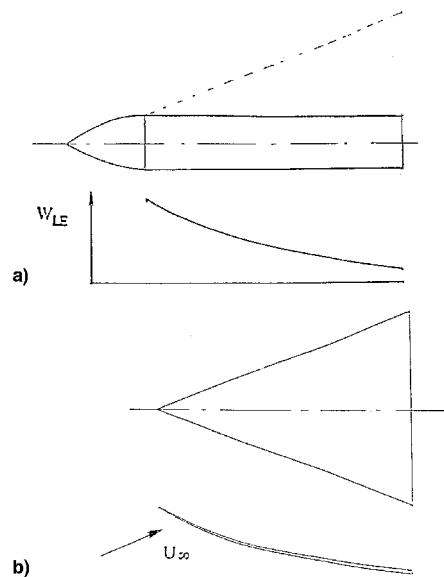


Fig. 4 Conceptual body-induced camber effect by a circular-cylinder body: a) upwash induced by body alone along the leading edge of planned delta wing geometry and b) equivalent cambered, planar, pure delta wing geometry.

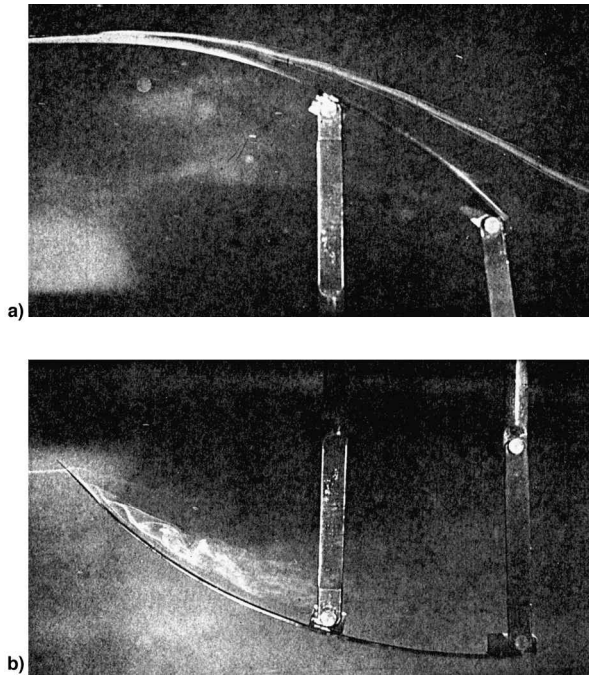


Fig. 5 Effect of static camber on delta wing vortex breakdown.⁸ Local incidence a) increasing and b) decreasing with distance from apex.

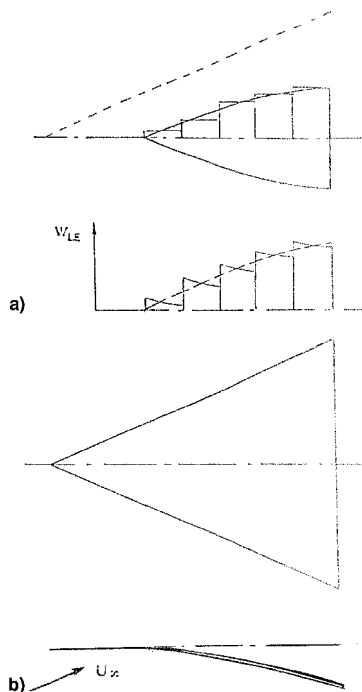


Fig. 6 Conceptual body-induced camber effect by an ogival centerbody: a) upwash induced by body alone along the leading edge of planned delta wing geometry, and b) equivalent cambered, planar, pure delta wing geometry.

mental results in Fig. 2, the positive forward camber effect dominated. This is understandable in view of the observed large effect of a drooping apex flap⁹ (Fig. 8). The improvement of the leading-edge vortex characteristics is obvious when comparing the pressure distribution under the vortex for the flap angle $B = 12$ deg with that for the basic wing, $B = 0$. In the conclusions of Ref. 9 it is revealed that "The deployment of an apex flap in a drooping position proved to delay the

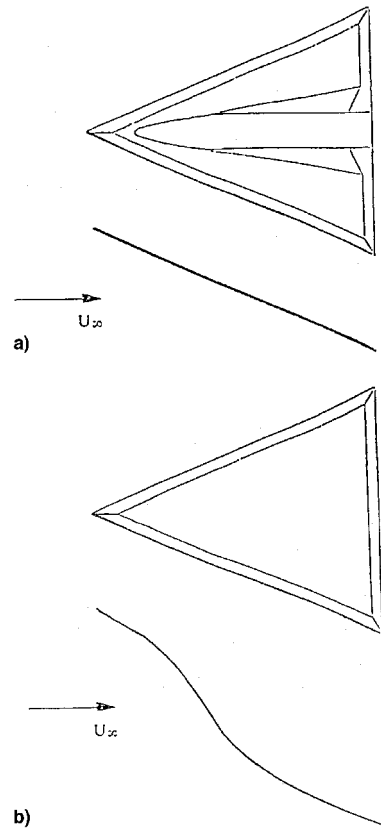


Fig. 7 Tested delta-wing-body geometry¹: a) fuselage with flat, planar wing, and b) conceptually equivalent cambered, planar wing alone.

appearance of breakdown over the wing to an angle of attack of about 8 deg beyond the corresponding value of the unmodified fixed wing." This is also the fuselage-induced effect at $\alpha = 30$ deg in Fig. 2b.

Based on the expected difference in body-induced camber effects for the area-changing and cylindrical parts of the fuselage, illustrated by the sketch in Fig. 7b, the presence of the centerbody should delay the breakdown travel toward the apex and accelerate the downstream travel toward the trailing edge. The experimental results³ in Fig. 2b show the expected speeding-up of the downstream travel toward the trailing edge with decreasing angle of attack to be more pronounced than for the pure delta wing.⁴ The body-induced slowdown of the breakdown travel toward the apex is also apparent when comparing the experimental results in Fig. 2b; the breakdown reaches the apex at $\alpha \geq 45$ deg for the delta-wing-body configuration compared with $\alpha < 35$ deg for the pure delta wings. The slowdown of the forward breakdown movement discussed in Ref. 10 cannot have been caused by a decrease of the effective angle of attack, as was suggested by the authors. At $\phi \neq 0$, the effective angle of attack and windward/leeward leading-edge sweeps are given by¹¹

$$\alpha(\phi) = \tan^{-1}(\tan \sigma \cos \phi) \quad (2)$$

$$\Lambda(\phi) = \Lambda \pm \tan^{-1}(\tan \sigma \sin \phi) \quad (3)$$

At $\phi = 14$ deg, Eq. (2) indicates that $\alpha(\phi)$ has decreased from 30 to 29.3 deg, barely enough to cause a noticeable change in breakdown position. However, the decrease of the windward leading-edge sweep to $\Lambda = 57$ deg should have promoted breakdown to reach the apex at $\alpha < 29.3$ deg.¹² Thus, the delay of the breakdown's arrival to the apex can only be the result of the forebody-induced camber-like effect (Fig. 7b),

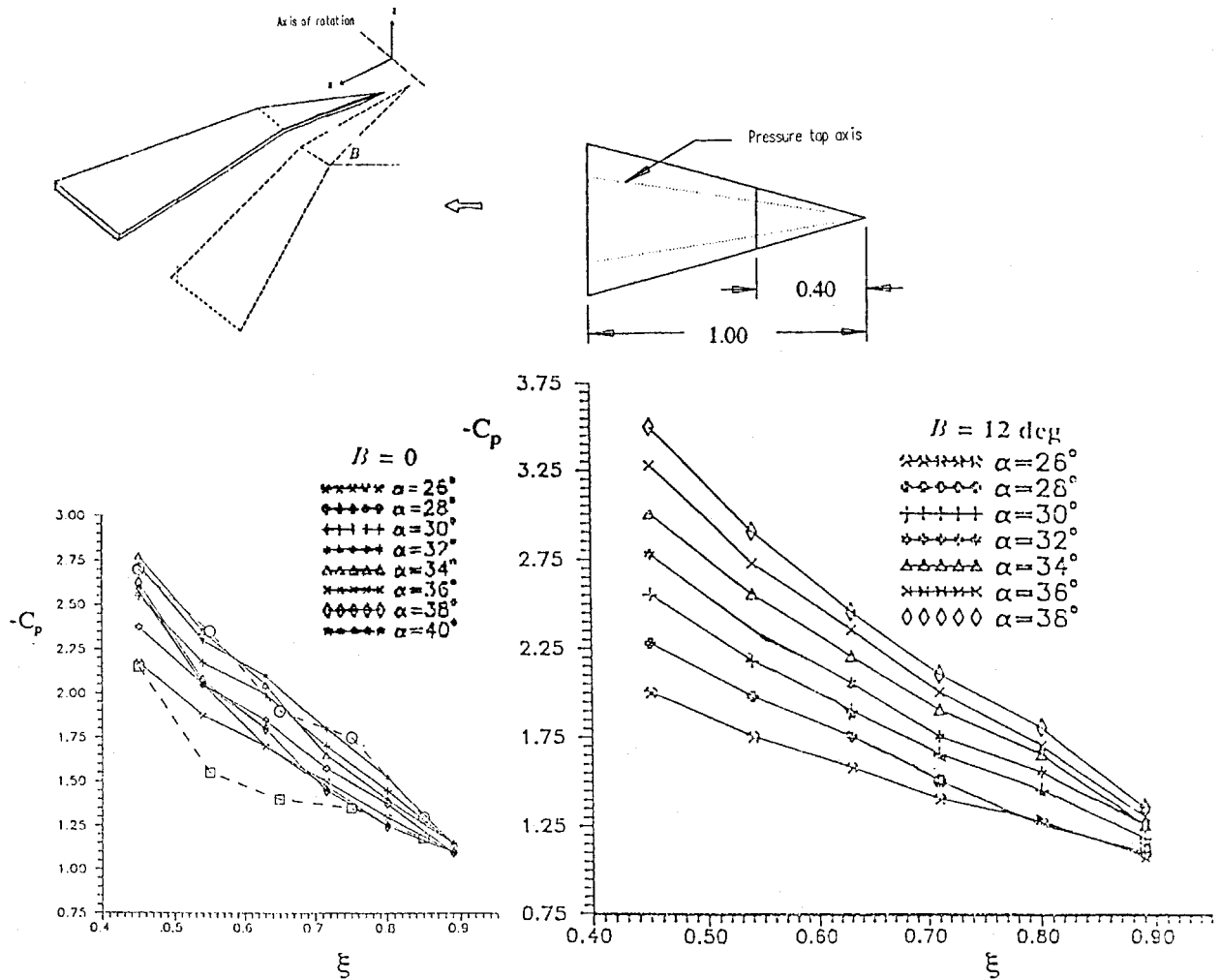


Fig. 8 Effect of delta-wing apex flap on vortex-induced pressure distribution.⁹

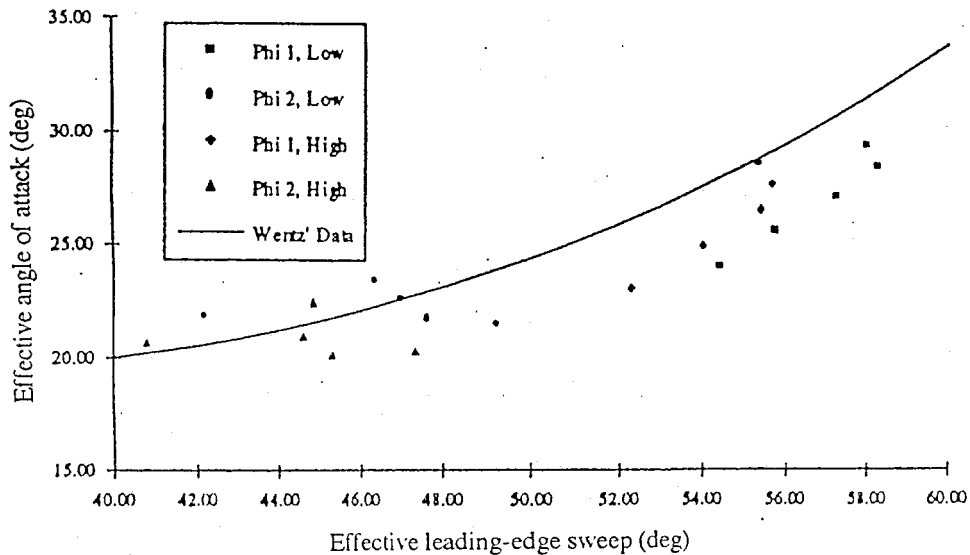


Fig. 9 Experimentally determined effective angle of attack and leading-edge sweep at which vortex breakdown reaches the apex on a rolling 65-deg delta-wing-body configuration.¹³

slowing down the breakdown travel forward to the nose of the centerbody. However, once past the nose, the breakdown should behave as on a pure delta wing. A detailed experimental investigation of this region¹³ showed that the measured occurrence of vortex breakdown at the apex correlated well with the Wertz-Kohlman results¹² (Fig. 9). The effective angle of

attack and leading-edge sweep are values adjusted for the effect of roll angle,¹¹ [Eqs. (2) and (3)]. The angle of attack was also corrected for the effect of $\delta_{LE} = 10$ deg, Ref. 5 and Eq. (1).

The experimental results in Fig. 9 were obtained when increasing the roll angle from $\phi = -30$ deg in increments of

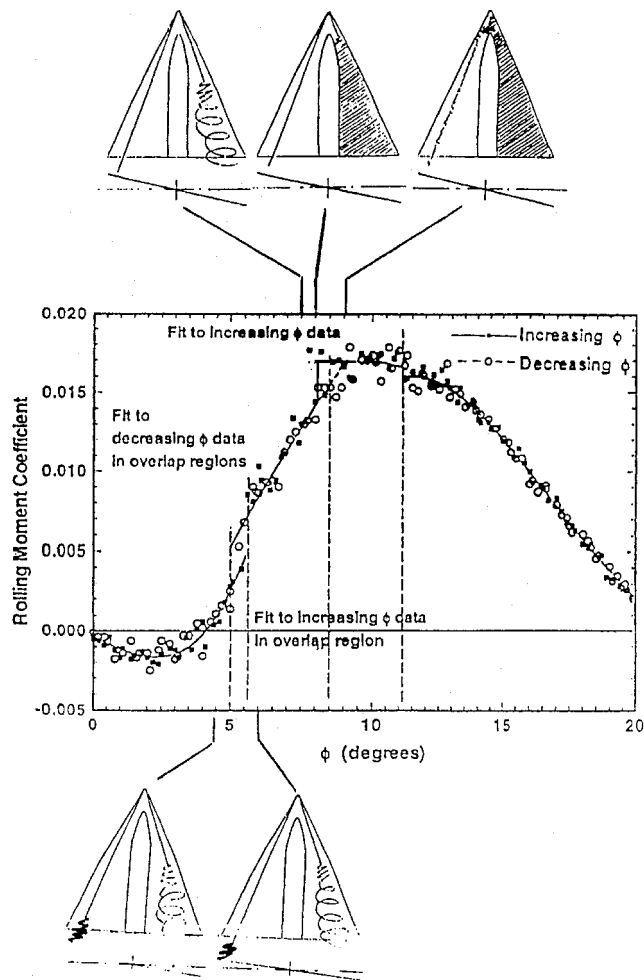


Fig. 10 Measured rolling moment at $\sigma = 30^\circ$ of a 65-deg delta-wing-body configuration as a function of roll angle.¹⁴

1–5 deg.¹³ The experimental data¹⁴ in Fig. 10, obtained for increasing and decreasing roll angles, show an interesting anomaly for the critical state at $\phi \approx 8.5^\circ$. Contrary to what was the case for the critical state at $\phi \approx 5^\circ$, no hysteresis loop of the usual type was measured at $\phi \approx 8.5^\circ$. According to Ref. 15, global flow separation occurs over the windward wing half when the roll angle is increased past $\phi = 8.5^\circ$, resulting in a discontinuous increase of C_l . However, when the roll angle is decreased, the return to the C_l level at $\phi < 8.5^\circ$ is not delayed, but instead promoted to occur at $\phi > 8.5^\circ$. This “presently unexplained anomaly” needs to be investigated further according to the authors of Ref. 14.

Because the critical state at $\phi \approx 5^\circ$ is generated by the travel past the trailing edge of vortex breakdown on the leeward wing half (bottom insets in Fig. 10), it is most likely not affected to any significant extent by the distant presence of the centerbody. Thus, earlier analyses^{16,17} still apply in this case. However, the critical state associated with the breakdown travel to the apex on the windward wing half (top insets in Fig. 10) is influenced dramatically by the presence of the body, an influence not considered in earlier analyses^{16,17} because this effect was unknown until the detailed measurements¹⁴ in Fig. 10 became available. The analysis in Ref. 17 assumed that the action creating the critical state at $\phi \approx 10^\circ$ took place when the breakdown on the windward side reached the apex, causing a sudden loss of lift generated by the helical flow downstream of a spiral vortex breakdown.^{18,19} The detailed measurements in Ref. 14 showed that this event took place already when the vortex breakdown approached the nose tip of the centerbody.

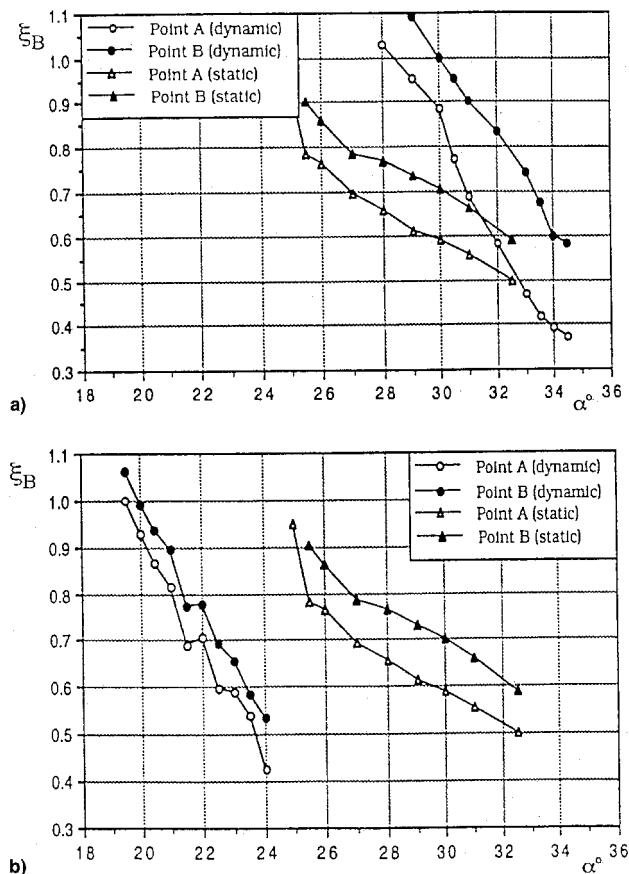


Fig. 11 Effect of rampwise α -change on the vortex breakdown on a 65-deg delta-wing-body configuration²³: a) increasing and b) decreasing angles of attack.

This is likely to have caused the measured C_l increase at $\phi \approx 8^\circ$. (Note that the local loads near the apex have no significant effect on C_l .) For increasing ϕ , this loss of downstream lift on the windward wing half is most likely the main contribution to the stepwise increase of C_l at $\phi \approx 8^\circ$.

When the roll angle is increased past $\phi = 8.5^\circ$, the vortex breakdown on the windward wing half advances until it is no longer prevented by the fuselage from interacting with the leeward side vortex flow near the apex. As the vortex is created at the apex, any interference with the process will affect the whole downstream development of the leeside leading-edge vortex, which itself does not burst on the wing until $\phi < 5^\circ$. This interference could have resulted in a less tightly wound vortex, as indicated in the top inset farthest right in Fig. 10, causing a loss of vortex lift on the leeward wing half that could be responsible for the sudden decrease of the $C_l(\phi)$ slope at $\phi > 8.5^\circ$. It was also most likely responsible for the large data scatter at $8.5 < \phi < 11^\circ$. The data set for decreasing ϕ indicates that the intermittent separation geometry illustrated in the top center inset in Fig. 10 could never be established. This is in general agreement with experimental results for double-delta²⁰ and straked-wing²¹ geometries. The dashed-line extension of the $C_l(\phi)$ slope from $\phi < 8.5^\circ$ in Fig. 10 illustrates how this would be recorded by the experimental results for decreasing ϕ . This fairing agrees with the measurements within the data scatter. When the roll angle is decreased below $\phi = 9^\circ$, the windward side vortex breakdown moves aft of the nose of the centerbody, which then can shield the leeward side vortex development from the interference generated by the windward side vortex breakdown. It should again be emphasized that the observed C_l changes are generated by the changes occurring in the downstream vortex-induced loads, and will, therefore, be associated with signifi-

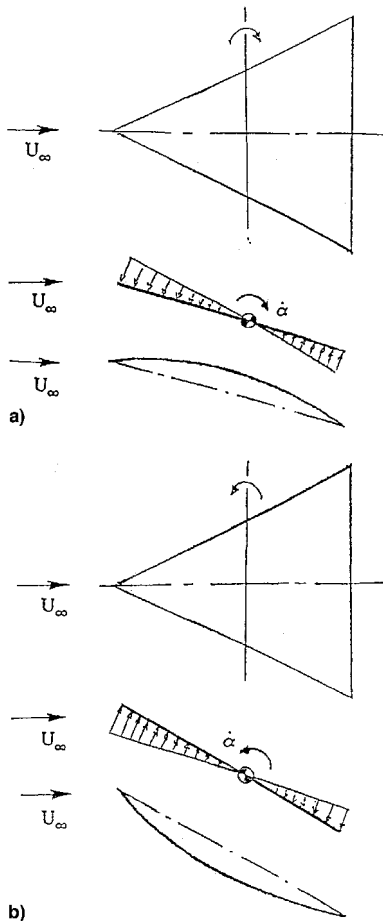


Fig. 12 Pitch-rate-induced camber effect: a) increasing and b) decreasing angle of attack.

cant time history effects. Recent experimental results²² have shown that the relaxation time (to 63% of steady-state C_l) is seven times larger for decreasing than for increasing roll angles through $\phi = 8$ deg. No such difference was observed for $\phi = 5$ deg, where vortex breakdown on one wing half cannot affect the vortical flow on the other half.

Other experimental results for the 65-deg delta-wing-body geometry²³ (Fig. 11) also demonstrate that the fuselage has a large effect on the unsteady vortex breakdown characteristics. (A and B denote the start and completion of vortex breakdown, respectively.) At $\xi > 0.40$, where the circular cross-sectional body promotes breakdown (Figs. 1 and 4), the pitch-rate-induced positive camber effect²⁴ during the upstroke (Fig. 12a) can delay vortex breakdown to occur as much as $\Delta\xi_B = 0.30$ behind the static location (Fig. 11a). However, the effect decreases rapidly when ξ_B approaches 40% chord, where the pitch-rate-induced positive camber (Fig. 12a) has to compete with the positive camber effect generated by the centerbody at $\xi < 0.40$ (Figs. 1 and 6). Conversely, during the downstroke (Fig. 11b), the pitch-rate-induced promotion of the occurrence of vortex breakdown on the wing²⁴ increases as ξ_B approaches 40% chord, where the pitch-rate-induced negative camber effect (Figs. 5b and 12b) no longer has to compete with the breakdown-promoting negative camber effect of the cylindrical cross-sectional afterbody (Figs. 1, 3, and 7).

The complex vortex breakdown aerodynamics for a pure delta wing are becoming significantly more complicated through the strong fuselage-induced effects discussed earlier. The silver lining of this problem is that the potential to delay vortex breakdown through careful fuselage design provides a powerful tool for improvement of the high-alpha performance of aircraft with delta wings. The fuselage shape of the tested model (Fig. 1), not specifically chosen for such a reason, still

appears to be at least as powerful in delaying vortex breakdown as a 12-deg deflected apex flap of 45% chordwise extent⁹ (Fig. 8).

The effects of a noncylindrical centerbody discussed earlier must be added to those discussed in Ref. 25 for cylindrical geometries when considering the use of a centerbody in ground facility tests of pure delta wings. The important task ahead is to get the technical community to appreciate the fact that the effect of a centerbody on delta wing vortex breakdown is anything but negligible.

Conclusions

An analysis of available experimental results from tests on delta-wing and delta-wing-body geometries has shown that a centerbody used to accommodate high-alpha tests of pure delta wings, as well as the fuselage on a delta-wing aircraft, can have a profound effect on the vortex breakdown characteristics, an effect that appears not to have been fully recognized until now.

References

- Hanff, E. S., and Jenkins, S. B., "Large-Amplitude High Rate Roll Experiments on a Delta and Double-Delta Wing," AIAA Paper 90-0224, Jan. 1990.
- Hanff, E. S., "Dynamic Non-Linear Air Loads Representation and Measurement," AGARD, CP-386, May 1985 (Paper 27).
- Huang, X. Z., and Hanff, E. S., "Leading-Edge Vortex Behavior and Surface Flow Topology," Workshop III, Delta-Wing Unsteady Aerodynamics and Modeling (Paper 2), AIAA AFM Conf., Aug. 1995.
- Lowson, M. V., and Riley, A. J., "Vortex Breakdown Control by Delta Wing Geometry," *Journal of Aircraft*, Vol. 32, No. 4, 1995, pp. 832-838.
- Ericsson, L. E., and King, H. H. C., "Effect of Cross-Sectional Geometry on Slender Wing Unsteady Aerodynamics," *Journal of Aircraft*, Vol. 30, No. 5, 1993, pp. 793-795.
- Straka, W. A., and Hemsch, M. J., "Effect of a Fuselage on Delta Wing Vortex Breakdown," *Journal of Aircraft*, Vol. 31, No. 4, 1994, pp. 1002-1005.
- Ericsson, L. E., "Comment on 'Effect of Fuselage on Delta Wing Vortex Breakdown,'" *Journal of Aircraft*, Vol. 31, No. 4, 1994, pp. 106, 107.
- Lambourne, N. C., and Bryer, D. W., "The Bursting of Leading-Edge Vortices—Some Observations and Discussion of the Phenomenon," Aeronautical Research Council, R&M 3282, England, UK, April 1961.
- Klute, S. M., Rediniotis, O. K., and Telionis, D. P., "Flow Control over a Maneuvering Delta Wing at High Angles of Attack," *AIAA Journal*, Vol. 34, No. 4, 1996, pp. 662-668.
- Huang, X. Z., Hanff, E. S., and Jobe, C. E., "Surface Flow Topology on a Delta Wing at High Incidence for a Range of Roll Angles," AIAA Paper 96-2398, June 1996.
- Ericsson, L. E., and Hanff, E. S., "Unique High-Alpha Roll Dynamics of a Sharp-Edged 65-Deg Delta Wing," *Journal of Aircraft*, Vol. 31, No. 3, 1994, pp. 520-525.
- Wentz, W. A., and Kohlman, D. L., "Vortex Breakdown on Slender Sharp-Edged Delta Wings," *Journal of Aircraft*, Vol. 8, No. 3, 1971, pp. 156-161.
- Addington, G. A., Hanff, E. S., and Nelson, R. C., "Leading-Edge Vortex Behavior in the Vicinity of a Delta Wing Apex," AIAA Paper 96-3388, July 1996.
- Jobe, C. E., Hsia, A. H., Jenkins, J. E., and Addington, G. A., "Critical States and Flow Structure on a 65-Deg Delta Wing," *Journal of Aircraft*, Vol. 33, No. 2, 1996, pp. 347-352.
- Huang, X. Z., Hanff, E. S., Jenkins, J. E., and Addington, G. A., "Leading-Edge Vortex Behavior on a 65° Delta Wing Oscillating in Roll," AIAA Paper 94-3507, Aug. 1994.
- Jenkins, J. E., Myatt, J. H., and Hanff, E. S., "Body-Axis Rolling Motion Critical States of 65-Degree Delta Wing," AIAA Paper 93-0621, Jan. 1993.
- Ericsson, L. E., "Flow Physics of Critical States for Rolling Delta Wings," *Journal of Aircraft*, Vol. 32, No. 3, 1995, pp. 603-610.
- Bergmann, B., Hummel, D., and Oelker, H.-Chr., "Vortex Formation over a Close-Coupled Canard-Wing-Body Configuration in Unsymmetric Flow," AGARD, CP-494, July 1994 (Paper 14).
- Ericsson, L. E., "Dynamic Stall of Pitching Airfoils and Slender

Wings—Similarities and Differences,” AIAA Paper 98-0414, Jan. 1998.

¹Ericsson, L. E., “Vortex Characteristics of Pitching Double-Delta Wings,” AIAA Paper 97-3574, Aug. 1997.

²Ericsson, L. E., and Beyers, M. E., “Nonlinear Rate and Amplitude Effects on a Generic Combat Aircraft Model,” AIAA Paper 98-0409, Jan. 1998.

²²Grismer, D. S., and Jenkins, J. E., “Critical State Transients for

a Rolling 65° Delta Wing,” AIAA Paper 2432, June 1996.

²³Huang, X. Z., and Hanff, E. S., “Unsteady Behavior of Spiral Leading-Edge Vortex Breakdown,” AIAA Paper 96-3408, July 1996.

²⁴Ericsson, L. E., “Pitch Rate Effects on Delta Wing Vortex Breakdown,” *Journal of Aircraft*, Vol. 33, No. 3, 1996, pp. 639–642.

²⁵Ericsson, L. E., and Beyers, M. E., “Ground Facility Interference Effects on Slender Vehicle Unsteady Aerodynamics,” *Journal of Aircraft*, Vol. 33, No. 1, 1996, pp. 117–124.